Thermal and spectroscopy studies of Ag$_2$SO$_4$ and LiAgSO$_4$

S. Rama Rao[1], Ch. Bheema Lingam[2, 3], D. Rajesh[2], R.P.Vijayalakshmi1, C. S. Sunandana[2]

[1]*Departmet of Physics, College of Sciences, Sri Venkateswara University, Tirupati 517502,*
[2]*School of Physics and 3ACRHEM, University of Hyderabad, Hyderabad 500 046, INDIA.*

Abstract: A comparative study is conducted on the structure, electronic and spectroscopic properties of Ag$_2$SO$_4$ and LiAgSO$_4$. Both the sulphates crystallise in an orthorhombic structure with the same space group of Fddd (70). A red shift in Raman modes indicates the stiffness of the crystal Ag$_2$SO$_4$ over LiAgSO$_4$. From ESR, it is observed that these sulphates has Mn^{2+} impurities leading to the g$_{av}$= 2.1040 at a field of 3255 G. This indicates that the Mn^{2+} ions have an environment close to octahedral symmetry. The g value corresponding to Ag$_2$SO$_4$ is 2.3005. The endothermic peaks in LiAgSO$_4$ at 388.8 and 420^{0}C are due to the formation of BCC structure of LiAgSO$_4$. The peak at 420.9^{0}C in Ag$_2$SO$_4$ may be due to the phase transition of β-Ag$_2$SO$_4$ particles to α-Ag$_2$SO$_4$ on heating.

I.   Introduction

Due to the single or successive reversible structural transitions for piezoelectric properties and high ionic conductivity of Alkali metal sulphates (Li$_2$SO$_4$, Na$_2$SO$_4$, K$_2$SO$_4$, Rb$_2$SO$_4$ and Cs$_2$SO$_4$) have attracted contemporary researchers [1-7]. The sliver and thallium based sulphate crystals are attractive due to the distinct conductivity behaviour of Ag+ and Tl+ [8-12]. The mixed sulphates such as AgLiSO$_4$, NaLiSO$_4$, RbAgSO$_4$, KLiSO$_4$ and TlAgSO$_4$ with two monovalent cations are known to be good solid electrolytes [11]. The fast-ion conduction in solids is a paradigm for structure-property relation. The structure factor can involve coordination geometry number, face-sharing sites in the structure and lattice disorder [13]. The structure of high conducting phase α- Ag$_2$SO$_4$ is isomorphous with that of the conducting phase Na$_2$SO$_4$ –I space group p63/mnc and both possess parallel properties linked to fast cation conductivity. The thermal properties are primarily interest due to their potential applications in electrochemical devices such as sensors [14]. A measurement of temperature depending on the electrical and thermal conductivities can serve as a useful tool in the study of ion transport in ionic crystals. Silver sulphate, a non-alkali metal sulphate, is an exception which shows high cationic conductivity inspite of the bigger size of Ag+. It undergoes a structural phase transition from the high temperature highly conducting hexagonal α-phase to the low temperature moderately conducting orthorhombic β-phase at 416^{0}C. It attracted scant attention until its application potential in SO$_x$(x=2, 3) galvanic sensors was proved [15]. Study on the role of electronic structure and the influence of lattice distortion caused by iso-valent cations on the mobility of Ag+ in orthorhombic β-Ag$_2$SO$_4$ is necessary to understand the fundamental conduction mechanism and simultaneously to obtain an apt silver sulphate based material for SO$_2$ gas sensor [16]. If silver sulphate diffuses into the battery electrolyte, metallic silver could get deposited on the negative plates. Fortunately, metallic silver has a relatively high hydrogen over-voltage, and contamination of the negative electrodes with small quantities of metallic silver should have only a minor effect on their self-discharge. Diffusion of silver sulphate into the battery electrolyte can be restricted by decreasing the diameter of the micro-fiber glass plug separator, by increasing its length and its density (compactness), and adding a gelling agent. On the basis of Fick's law, one can estimate that it should be possible to limit the diffusion into the battery electrolyte (at 258^{0}C) to less than 0.1 mg of metallic silver per year [17]. New solid-state electrochemical sensors using Li$_2$SO$_4$-Ag$_2$SO$_4$ solid electrolytes have been recently developed to measure SO$_2$ and/or SO$_3$ in gas mixtures. The sensors which consist of a two-phase electrolyte and a solid Ag-(Ag$_2$SO$_4$) reference electrode exhibit excellent behaviour. For example, they have long-term electrochemical stability and accurate potentiometric responses are obtained over a six month period. The presence of significant concentrations of CO$_2$ and H$_2$0 in the gas mixture has no effect on the sensor response. Thus these sensors have potential applications as reliable detectors and monitors of SO$_2$ and/or SO$_3$ concentrations in various gaseous atmospheres[18-20]. For the equimolar compositions of the two phases the electrical conductivity and the diffusion coefficients of Li+, Ag+ and Na+ at 823K are nearly the same for the two abundant cations, while they are considerably smaller for the cation that is present at low concentration. Additional evidence that the two abundant cations have nearly the same mobility in the bcc phase is obtained from a trans- port number study for (Li, Ag)$_2$SO$_4$ [21-24].

II. Experimental

2.1 Synthesis

The materials used in this experiment Li$_2$SO$_4$.H$_2$O (Alfa) and Ag$_2$SO$_4$ (AR) were been mixed in 1:1 ratio and grinded for one hour in a agate mortor and then transferred to heater. The powder is heated at 200°C for 10 hours, and subsequently cooled to room temperature. LiAgSO$_4$ was again thoroughly grinded and used for further characterization.

2.2 Instrumentation

The crystal structure of the samples was characterized by X-ray powder diffractometer using Co Kα radiation (λ = 1.7889 Å). The morphologies and chemical composition of these samples were obtained by Field emission scanning microscopy (FESEM) and for chemical composition using energy dispersive X- ray scattering (EDS) analysis (a model no ULTRA- 55, ZEISS, Japan).Raman spectra were recorded at 300K in a backscattering geometry with Horiba JobinYvon, LabRAM- HR800 micro-Raman system using 514.5 nm excitation from Ar+ gas laser. The differential scanning calorimetry (DSC) was done using DuPont 9900 model DSC instrument. Finally, the electron spin resonance spectra (EPR) were recorded on a JEOL9FE-3X) X-Band spectrometer under optimized conditioned of modulation amplitude, receiver gain, time constant and scan time.

III. Results And Discussion

3.1 Structure and morphology

The structure and morphology of Ag$_2$SO$_4$ and LiAgSO$_4$ are studied using XRD and FESEM-EDS, the corresponding XRD pattern is given in Figs.1 and 2. From Fig.1A, the XRD pattern of Ag$_2$SO$_4$ is identified as orthorhombic (a= 5.817, b=12.70 and c=10.269) with the space group of Fddd (70). The diffraction peaks observed from XRD are (040), (202), (331), (151), (511), (260), (602), (642), (800), and (084). The peaks (602) and (800) are found to be high intensive. The obtained XRD pattern matches well with the standard data (JCPDS card no. 07-0203) as reported here in. Whereas, the XRD pattern (see Fig.2A) of LiAgSO$_4$ is also identified as orthorhombic (a=10.25, b=12.69 and c=5.843). The diffraction peaks from XRD are observed as (200), (040), (311), (022), (202), (331), (151), (351), (062), (080), (333), (371), and (602). The peak (220) is found to be high intensive. The obtained XRD pattern matches well with the standard data (JCPDS card no. 52-1211). The structure details of Ag$_2$SO$_4$ and LiAgSO$_4$ are in good agreement with the previous studies. Then the morphology and surface characteristics of Ag$_2$SO$_4$ and LiAgSO$_4$ are understood from the FEMSEM. LiAgSO$_4$ samples have nano particles with the average size of 100-120 nm which is shown in Fig.2B. In the case of Ag2SO4, the average particle size is found to be 10-20 nm (see Fig.1B). The elemental analysis of LiAgSO$_4$ and Ag$_2$SO$_4$ samples was determined by using EDS technique. The EDS clearly shows the formation of Ag, O and S elements, formation of LiAgSO$_4$ and Ag$_2$SO$_4$ and the EDS analysis confirms that the chemical composition of LiAgSO$_4$ and Ag$_2$SO$_4$ is almost in stoichiometric ratios.

3.2 Raman Spectroscopy and phase transition

The obtained Raman spectra of LiAgSO$_4$ and Ag$_2$SO$_4$ are shown in Fig.3A. One external mode is observed in both the spectra, in accordance with the model that the high- conducting solid phases with reorienting sulphate ions. The spectra look similar to those of the melts, which is a general finding for superionic materials. The observed mode frequencies for LiAgSO$_4$ and Ag$_2$SO$_4$ are ν_1, ν_2, ν_3 and ν_4 which are basically from sulphate –ion intermolecular vibrations. Furthermore, the mode frequencies of solid phases agree with previous calculations [18-25]. This confirms our synthesis and structure of the LiAgSO$_4$ and Ag$_2$SO$_4$. We observed 91.6 cm^{-1} as ν_{ext}. The intense peak at 970 cm^{-1} is denoted as ν_1, whereas 427 and 457 cm^{-1} are under the ν_2 band. The peaks 1007 cm^{-1} and 1045 cm^{-1} are ν_3 band. The ν_4 consists of 623 cm^{-1} mode. ν_1 and ν_4 modes decreases with increasing size of the alkali metal cations. By comparing with Raman spectra of Ag$_2$SO$_4$, it is observed that the intensity of ν_2 and ν_4 bands decreases i.e they are inactive. Whereas the intensity of ν_3 band increases i.e it is active. The intensity of ν_1 band remains same.

3.3 Differential Scanning calorimetry

A typical DSC curve of heat flow vs sample temperature consists of a series of peaks measured against a standard sample (Iridium) in upward as well as downward direction. The position, shape and the number of peaks will help in identifying the thermal events occurring in the substance. More importantly, since the areas under the peaks are related to the enthalpy of transmission, these facts are used for quantitative determination of thermodynamic quantities. Any phenomenon that produces enthalpy changes or change of heat capacity is denoted by DSC. Physical changes in solids may involve evolution or absorption of heat. This is viewed in DSC as an exothermic or endothermic peak. A transition such as melting or a structural phase transition yields an endothermic, while an amorphous to crystalline transition gives an exothermic. DSC analysis of the Ag$_2$SO$_4$ and LiAgSO$_4$ is carried out at the heating rate 10C/min up to 600^{0}C as shown in Fig.3B. A strong H$_2$O peak present

at 141.13 in LiAgSO$_4$, interestingly it is not found in Ag$_2$SO$_4$. The small endothermic peaks in LiAgSO$_4$ at 388.8 and 420^{0}C are due to the formation of BCC structure of LiAgSO$_4$. Knowing that a mechanical mixture cannot be absolutely homogenous, the small endothermic peak at 515.9^{0}C is observed in LiAgSO$_4$. And the thermal effect starting at 542.8^{0}C is purely from the melting point of the BCC LiAgSO$_4$. The peak at 420.9^{0}C in Ag$_2$SO$_4$ may due to the phase transition of β-Ag$_2$SO$_4$ particles to α-Ag$_2$SO$_4$ on heating. On heating, the excess heat flow at the structural transition was recorded as DSC signal by S.W.Tao et al noticed two small anomalies at 427.7C and 567.9^{0}C. It was found that the anomaly depended on the turning temperature at which a cooling run was changed to a heating run [22].

3.4 Electron spin resonance

Electron spin resonance is a specific microscopic probe to examine molecular environments in crystalline and disordered systems. Under favourable circumstances, it is possible to create and stabilize paramagnetic radicles which may reflect certain aspects of dynamics- which may be characteristic of the system itself. Presently we describe our efforts to stabilize and identify molecular paramagnetic radicles in Ag$_2$SO$_4$ and LiAgSO$_4$. The ESR spectra of Ag$_2$SO$_4$ and LiAgSO$_4$ are shown in Figs.3C and D. The ESR signals suggesting a common origin for the paramagnetic centres are involved. In the spectra of LiAgSO$_4$, we observed six sharp peaks almost with equal spacing 98 G. These are due to Mn^{2+} impurity present in LiAgSO$_4$. The g$_{av}$ = 2.1040 at a field of 3255G and g$_{cen}$ = 2.1238 at a field 3219.9 G. This is due to the presence of Mn^{2+} ions in an environment close to octahedral symmetry. The g value corresponding to Ag$_2$SO$_4$ is 2.3005.

3.5 Fourier Transform Infrared Spectroscopy

In order to get some structural information of Ag$_2$SO$_4$ and LiAgSO$_4$ solid solution, IR absorption spectra of a mechanically mixed powder are shown in Figs.4A and B. The free sulphate SO$_4^{2-}$ ion belongs to the high symmetry point group. For LiAgSO$_4$, four fundamental internal vibration modes are observed; the symmetric stretching mode ν$_1$ and the doubly degenerate symmetric bending mode ν$_2$ are IR inactive. The asymmetric stretching mode ν$_3$ and ν$_4$ are both triply degenerate and IR active. The spectra show an increase of IR transmission, inactive absorption ν$_1$ around 619.18 cm^{-1} and ν$_2$ is around 997.26 cm^{-1}. More over the broadening of the IR active absorption ν$_3$ around 1112.33 cm^{-1} and ν$_4$ around 646.58 cm^{-1} indicates the decrease in symmetry of the SO$_4^{2-}$ ions due to the incorporation of Li$^+$ ions in to the interstitial positions and/or Ag$^+$ lattice sites, resulting in the change of structural environment. That is, IR spectra indirectly demonstrate the formation of LiAgSO$_4$ phase. The higher order modes are due to the presence of H$_2$O, which are belongs to O-H vibrations. For Ag$_2$SO$_4$, only two modes are observed at 991.78 and 1128.77 cm^{-1}.

IV.   Conclusions

A comparative study conducted on the structure, electronic and spectroscopic properties of Ag$_2$SO$_4$ and LiAgSO$_4$ is reported. Both the sulphates crystallised in orthorhombic structure with the same space group of Fddd (70). A red shift in Raman modes indicates the stiffness of the crystal Ag$_2$SO$_4$ over LiAgSO$_4$. From ESR, it is observed that these sulphates have Mn^{2+} impurities leading to the g$_{av}$= 2.1040 at a field 3255 G. This is due to Mn^{2+} ions in an environment close to octahedral symmetry. The g value corresponding to Ag$_2$SO$_4$ is 2.3005. The endothermic peaks in LiAgSO$_4$ at 388.8 and 420^{0}C are due to the formation of BCC structure of LiAgSO$_4$. The peak at 420.9^{0}C in Ag$_2$SO$_4$ may due to the phase transition of β-Ag$_2$SO$_4$ particles to α-Ag$_2$SO$_4$ on heating.

References

[1]. Zengcai, L.; Wujun, Fu.; Andrew Payzant E.; Xiang, Y.; Zili, Wu.; Nancy J. D.; Jim, K.; Kunlun, H.; Adam J. R.; Chengdu, L.; *J. Am. Chem. Soc.,* **2013**, *135,* 975–978.
[2]. Yusheng, Z.; Luke L. D.; *J. Am. Chem. Soc.*, **2012**, *134,* 15042–15047.
[3]. Hisashi, K.; Kazushige, O.; Kunihito, K.; *Inorg. Chem.*, **2012**, *51,* 9259–9264.
[4]. Radhakrishnan A. N.; Prabhakar Rao, P.; Mahesh, S. K.; Vaisakhan Thampi D. S.; Peter, K.; *Inorg. Chem.*, **2012**, *51,* 2409–2419.
[5]. Molenda, J.; *Func. Mat. Lett*, **2011**, *4,* 107-112.
[6]. Xin-Xing, Z.; Min L.; *J. Phys. Chem. Lett.*, **2013**, *4,* 1205–1210.
[7]. Singh, K.; Bhoga, S. S.; *Bull. Elctrochem.* **1996**, *12,* 633-642.
[8]. H. Kasano, S. Tsuchiyama, Y. Kawamura, H. Mashiyama, Ferroelectrics, 1998, 217, 121-128.
[9]. H. Mashiyama, J. Wu, F. Shimizu and M. Takashige, Physical society of Japan 1998, 67, 359-360.
[10]. C. Ramasastry, C.S. Sunandana, B.S.V.S.R. Acharyulu, J Nonmetals, 1972, 1, 283-290.
[11]. Y. Lu, E.A. Secco Solid State Ionics 53-56,223 (1992).
[12]. A. Elfakir, J. Souron, G. Wallez, M. Quarton, M. Touboul, Solid State Ionics, 1998, 110, 145-151.
[13]. R. A. Secco, E. A. Secco, J. Phys. Chem. Solids, 1995, 56, 1045-1051.
[14]. HirotoTomica and Sadao Adachi J. of Solid State Science and Technology 2(6) 253-258 (2013).
[15]. S.W. Anwane ADV. Mat Letters 3(3). 204-212 (2012).
[16]. Singh, AnwaneS.W,Bhoga.S, Solid State Ionics 187,86-87 (1996).
[17]. PaulRuetschi J. Power Sources 116, 53-60 (2003).
[18]. L. Borjessand L.M. TorellPhysica Rev B 32,4 (1985).
[19]. Q.G. LIU and W.L. WORRELLSolid StateIonics 18 & I9 (1986) 524-528 524.

[20]. Tiwari, A.; Mishra, A.K.; Kobayashi, H; Turner, P F; IntelligentNanomaterials Wiley-Scrivener Publishing LLC, USA, 2012 ISBN 978-04-709387-99(2012).
[21]. S. W. AnwaneAdv. Mat. Lett.4(4), 300-309 (2013).
[22]. S.W. Tao, X.Q. Liu, D.K. Peng, G.Y.Meng Material Letters 34, 30-35 ((1998).
[23]. Irene Martina, Rita Weisinger, DubravkaJembrih- Simburger Manfred Schreiner Micro- RamanSpectroscopy of Silver Corrosion products e-ps 9, 1-8 (2012).
[24]. Leif NILSSON and N.Hessel ANDERSENSolid State Ionics 34, 111-119(1989).
[25]. Roy Theberg, Arnold LundenSolid State Ionics 90 , 209-220(1996).

Figure captions

Fig.1. The (A) X-ray diffraction, (B) FESEM and (C) EDS of Ag₂SO₄.

Fig.2. The (A) X-ray diffraction, (B) FESEM and (C) EDS of LiAgSO₄

Fig.3. (A) Raman spectroscopy, (B) DSC and (C), (D) ESR of Ag₂SO₄ and LiAgSO₄

Fig.5. FTIR of (A) Ag₂SO₄ and (B) LiAgSO₄.

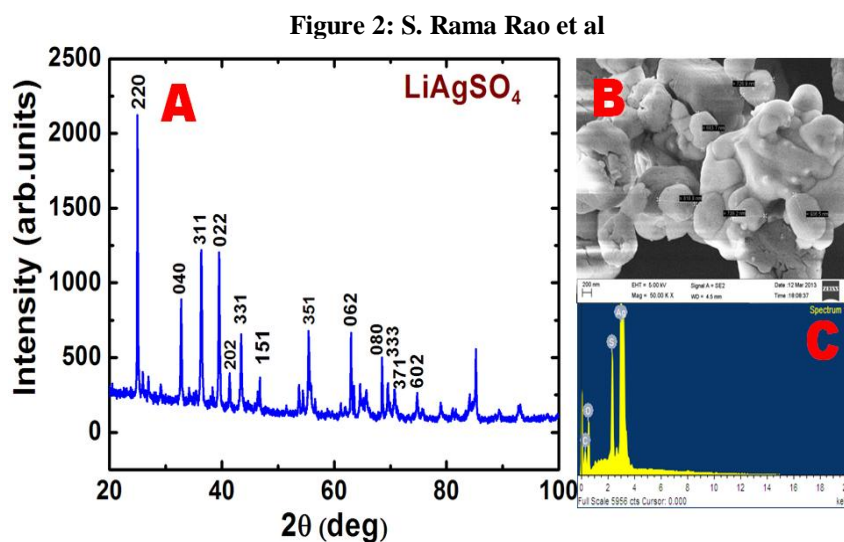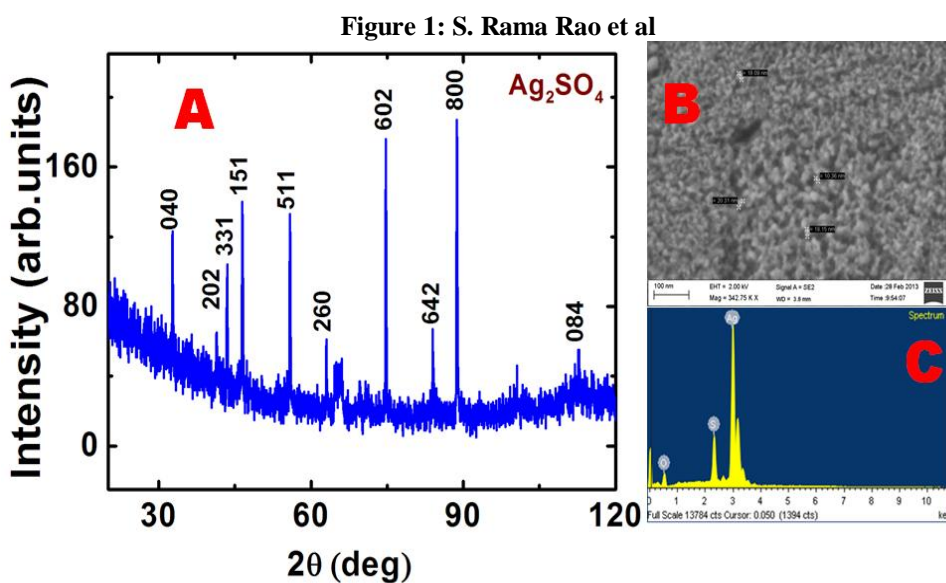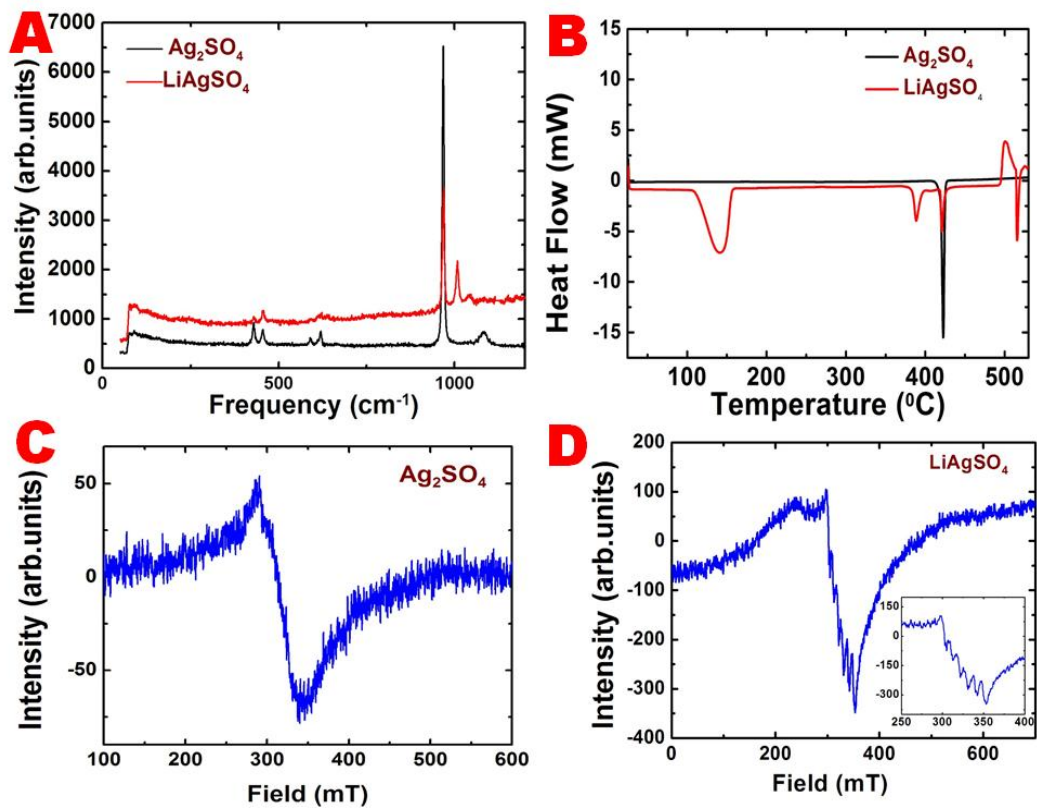**Figure 1: S. Rama Rao et al**

Figure 2: S. Rama Rao et al

Figure 3: S. Rama Rao et al

Figure 4: S. Rama Rao et al